Fluoride degradable and thermally debondable polyurethane based adhesive

Article

Accepted Version

Singh Babra, T., Trivedi, A., Warriner, C. N., Bazin, N., Castiglione, D., Sivour, C., Hayes, W. ORCID: https://orcid.org/0000-0003-0047-2991 and Greenland, B. W. (2017) Fluoride degradable and thermally debondable polyurethane based adhesive. Polymer Chemistry, 8 (46). pp. 7207-7216. ISSN 1759-9954 doi: 10.1039/C7PY01653K Available at https://centaur.reading.ac.uk/73806/

Fluoride degradable and thermally debondable polyurethane based adhesive.

Tahkur Singh Babra,[a] Akash Trivedi,[b] Colin N. Warriner,[c] Nicholas Bazin,[c] Dario Castiglione,[c] Clive Sivour,[b] Wayne Hayes,[c] Barnaby W. Greenland.[e*]

[a] Reading School of Pharmacy, University of Reading, Whiteknights, Reading, RG6 6AD (UK) email: b.w.greenland@reading.ac.uk

[b] Department of Engineering Science, University of Oxford, Parks Road, Oxford, OX1 3PJ (UK)

[c]AWE Plc, Aldermaston, Reading, Berkshire, RG7 4PR (UK)

[d]Department of Chemistry, University of Reading, Whiteknights, Reading, RG6 6AD (UK)

[e]Department of Chemistry, University of Sussex, Falmer, BN1 9QJ, UK

email: b.w.greenland@sussex.ac.uk

Abstract

We report the one-pot, solvent free synthesis of a stimuli-responsive polyurethane (PU) adhesive. The hard domains within the supramolecular PU network contain a silyl protected phenol 'degradable unit' (DU). The DU undergoes rapid decomposition (<30 minutes) upon treatment with fluoride ions which causes depolymerisation of the linear PU adhesive. The mechanism of depolymerisation was investigated in solution using ^{1}H NMR spectroscopy by following the degradation of the polymer in the presence of *tetra*-butylammonium fluoride (TBAF). In the absence of fluoride ions, the material behaves as a typical thermoplastic adhesive, and underwent four adhesion/separation cycles without loss of strength. The fluoride initiated depolymerisation of the PU adhesive in the solution state was verified by GPC

analysis, showing reduction in M_n from 26.1 kgmol^{-1} for the pristine PU to 6.2 kgmol^{-1} for the degraded material. Degradation studies on solid samples of the PU which had been immersed in acetone/TBAF solution for 30 minutes exhibited a 91 % reduction in their modulus of toughness (from 27 to 2 MJ m^{-3}). Lap shear adhesion studies showed the fluoride responsive PU was an excellent material to join metallic, plastic, glass and wood surfaces. Pull adhesion tests confirmed that immersing the adhesive in TBAF/Acetone solution resulted in a reduction in strength of up to 40% (from 160 N to 95 N at break) after drying.

Introduction

Materials with applications as adhesives, sealants and coatings are a vibrant area of polymer chemistry.[1] This scientific interest in this field is driven by the industrial importance of the products which include hot melt adhesives,[2–8] hydrogels,[9–13] epoxy resins[6,14–17] and cross-linked adhesives.[18–20] A more recent addition of this research field is the study of responsive adhesives. These materials are able to debond in response to a stimulus, or can exhibit reversible properties which allow for multiple adhesion/separation/adhesion cycles without loss of strength. Responsive adhesives are finding an ever-expanding market, where they replace traditional fabrication methods such as riveting or welding, yet permit easy disassembly of the component at the end of its lifecycle. This class of adhesive are becoming increasingly important in order to facilitate more rapid and cost effective recycling of key components and materials.

The externally controlled temporary reduction in tensile modulus and/or adhesion strength has been demonstrated for various systems, for example, in supramolecular materials or those containing dynamic covalent bonds.[21] This progress in bottom-up material design has facilitated the immergence of new technologies[22,23] across a broad range of disciplines including biomedical applications,[24–27] sensors,[28] healable[29] and damage sensing materials[30] as well as improving product recyclability.[25,31,32]

With respect to reversible adhesive materials, dynamic covalent chemistries[21] have, to date, received the most attention. Typically, these materials break down from high strength to low strength networks on application of a suitable external stimulus (e.g. heat/ light). Removal of that stimulus can lead to a restoration of the pristine properties of the material. This was recently shown by Rowan *et al.* who produced a reversible adhesive harnessing the dynamic nature of the disulfide bond when irradiated with high intensity UV light.[29] Aubert *et al.* produced a debondable epoxide based adhesive which made use of the thermo-reversible (110 °C) formation of the Diels-Alder adduct formed between furan and maleimide.[14] Weder and co-workers synthesised an aliphatic azo containing polymer, which breaks down with either heat or high intensity UV light, weakening the material.[33] Bao and co-workers showed the use of a reversible boroxine bond, which breaks by hydrolysis or force and but can reform by loss of water.[34]

A conceptually distinct class of polymeric adhesive that can debond on command are those that contain supramolecular non-covalent interactions which form a reversible network.[35] Thermo-responsive supramolecular adhesives utilising hydrogen bonding[22,36–41] have been demonstrated, in addition to those that harness metal/ligand interactions which were responsive to both light and heat.[22]

An additional functionality that can be built into these systems is the ability to undergo a permanent reduction in tensile modulus/adhesion strength which persists after the stimulus has been removed. This could be achieved by using a depolymerisation material that undergoes an irreversible reduction in molecular weight leading to a permanent reduction in strength. This was recently demonstrated by Phillips and co-workers who designed an adhesive that degrades on contact with fluoride ions.[42] In this system, fluoride ions caused degradation of an intractable, crosslinked material resulting in a dramatic weakening of the adhesive.

Herein we present the design and synthesis of a chemo-responsive depolymerisable hot melt adhesive. In contrast to the previous crosslinked fluoride responsive systems, this novel linear polyurethane (PU) behaves as like a typical reversible adhesive, undergoing multiple break/readhesion cycles without loss of bonding strength (Scheme 1). However, the PU also contains multiple fluoride responsive depolymerisable units in the main chain. Contact with fluoride ions results in a permanent reduction in molecular weight and consequently a reduction in the strength of the bond between the components without further application of the stimulus. This approach enables this system to be: i) multi-stimuli responsive, exhibiting reversible adhesive properties in response of one stimuli and permanent loss of adhesion in response to a second stimuli and ii) chemo-responsive in nature to permit use in situations where other stimuli including heat or light cannot be used, for example for disassembly of thermally sensitive components, or those that are not transparent at the appropriate wavelength of radiation.

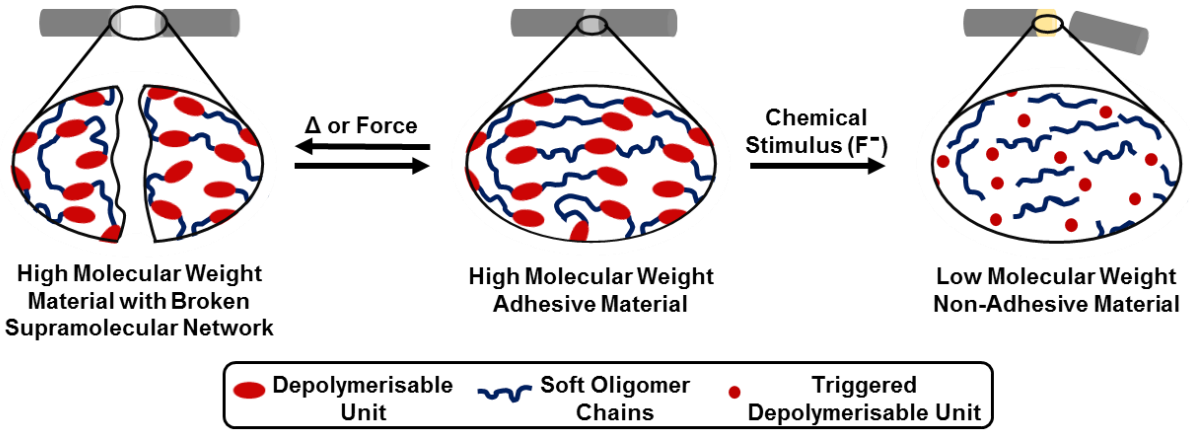

Scheme 1 *Schematic showing the rebondable nature of the adhesive in response to elevated temperatures, and complete non-reversible depolymerisation in response to fluoride ions.*

Results and Discussion

Previously, Akkaya and co-workers[43] have shown that *tert*-butyl dimethylsilyl (TBDMS) protected cresol **2**, synthesised by a two-step process, can be reacted with dioxetane to produce a biscarbonate. This species can undergo fluoride initiated degradation of the carbonate functionalities accompanied by loss of CO_2. In addition, Shabat showed the enzyme triggered degradation of a carbamate functionalised cresol as part of an amplified drug release molecule.[44] Inspired by these works, we synthesised the novel silyl protected biscarbamate (**3**) from the degradable unit (DU) **2** (Scheme 2). We envisioned **3** would be a chemically representative model compound for a small section of the backbone of a fluoride degradable PU system.

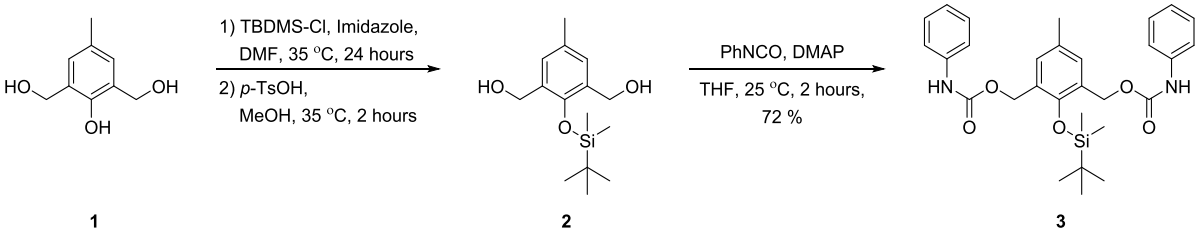

Scheme 2 *Synthesis of the degradable unit (**2**) and model bisurethane compound (**3**).*

Before synthesising polymers and testing complex polyurethane systems, it was first important to demonstrate the selective response of the DU **2** to fluoride ions. A model bisurethane compound (**3**, Scheme 2) was synthesised using phenyl isocyanate end groups. Addition of fluoride ions in solution resulted in complete degradation of the system in less than one minute as observed by ^{1}H NMR and UV/vis spectroscopy (see supplementary information (SI), S1). Model compound **3** was found to be stable in solution on contact with other halide ions including chloride, bromide and iodide (SI, S1). Furthermore, a second model bisurethane compound containing a methoxy group rather than the TBS group of **3** was synthesised.

Addition of fluoride ions to this methoxy analogue did not result in degradation, showing the TBS group was vital to the correct functioning of this DU (see SI, S2).

These experiments demonstrated that degradation was initiated by selectively by fluoride ions, and confirmed the suitability of **2** as the responsive degradation unit in PU-type polymeric architectures.

Polymer Synthesis

With the synthesis and selective degradation of the novel fluoride selective DU evaluated, attention turned to the synthesis of the responsive PU adhesive. This was synthesised using a one-pot, two step synthesis.[45–47] Initially, an isocyanate terminated pre-polymer **6** was produced by addition of methylene diphenyl diisocyanate (MDI) **5** to Krasol HLBH-P 2000 (Krasol) **4** at 80 °C (Scheme 3). After 3 hours, the DU **2** was added and the temperature increased to 100 °C, (melting point of **2** is 93 - 95 °C) and the resulting homogeneous mix stirred until it solidified to give the crude polymer (Scheme 3).

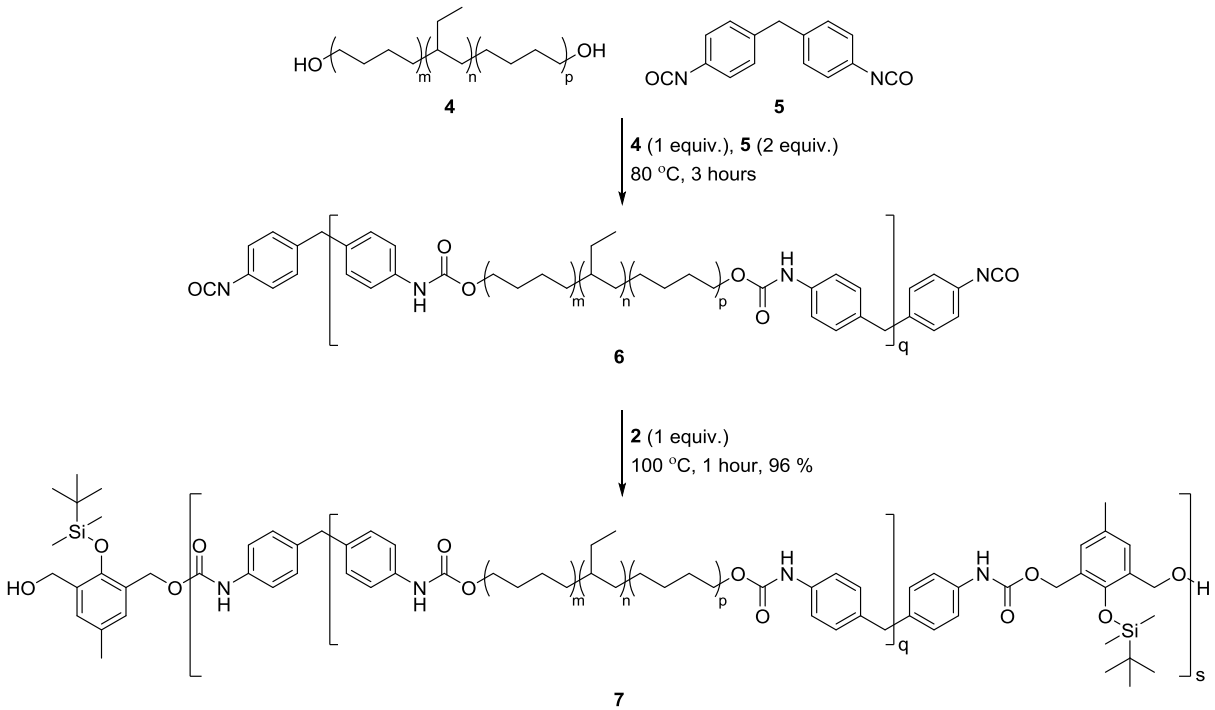

Scheme 3 *Solvent free synthesis of the adhesive polymer using Krasol, MDI and the DU (q = 1, 2; s = 8).*

GPC analysis of polymer **7** revealed essentially monomodal distribution with M_w 71400 $gmol^{-1}$, M_n 26100 $gmol^{-1}$ and $Đ$ 2.73, indicating that significant chain extension occurs during the reaction (Krasol **4** = M_w 3700 $gmol^{-1}$, M_n 3300 $gmol^{-1}$).

The thermal properties of the material were studied using differential scanning calorimetry (DSC) and dynamic mechanical analysis. DSC of the polymer showed a glass transition temperature (T_g) at *ca*. -45 °C, which is similar to that of the starting Krasol (T_g *ca*. -46 °C), and is indicative of a phase separated material. The T_g was unaltered over 3 heat/cool cycles showing thermoreversible nature of the material. No polymer melt was seen in the DSC data confirming the amorphous nature of the material.

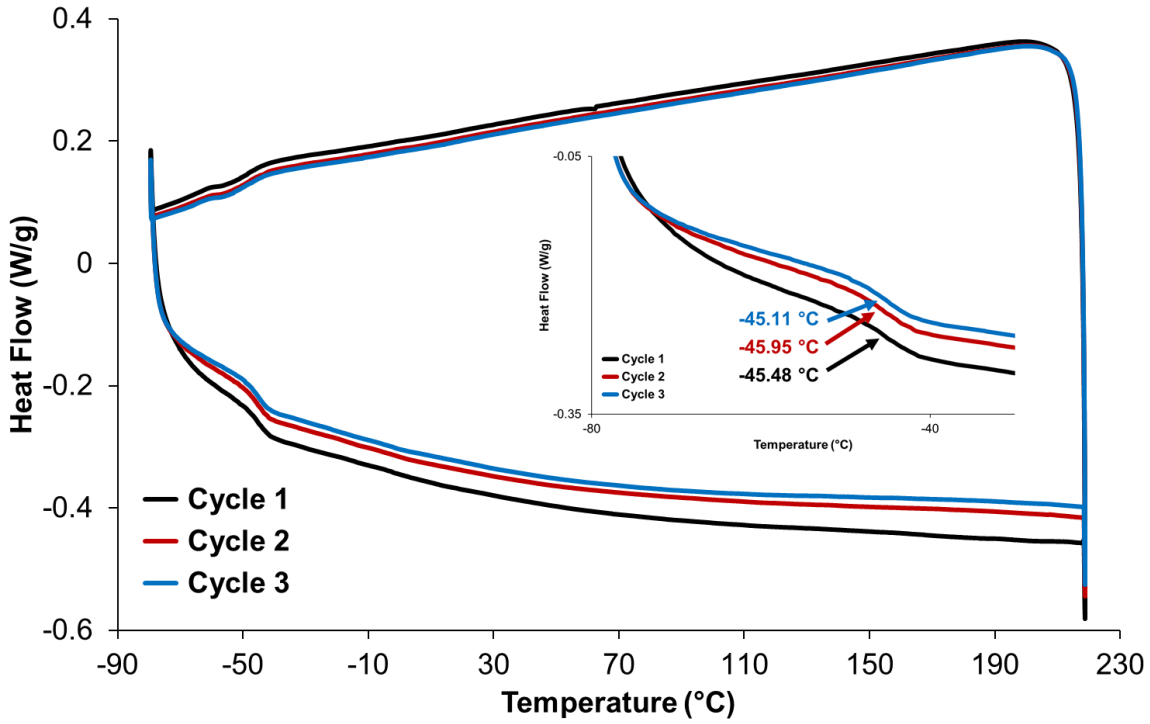

Figure 1 *DSC thermogram of the three heat – cool cycles of Polymer* ***7****. Insert shows glass transitions from each cycle. See SI, S3 for raw data.*

Polymer **7** was subject to dynamic mechanical analysis (DMA, see SI, S4) and rheological testing (Figure 2) to further investigate the thermomechanical response of the material. In the DMA data, a phase transition was observed at approximately -45 °C, indicating the glass transition temperature and agreeing with the DSC results. A sharp decrease in both storage and loss modulus was observed at temperatures between the T_g and -30 °C, followed by a gradual decrease until specimen failure at 87 °C. Rheological data were obtained at temperatures up to 150 °C. A viscoelastic transition was observed at approximately 128 °C at which the storage and loss moduli cross-over. This remained constant with the three cool-heat cycles (Figure 2). These data clearly show the thermo-reversible nature of the material.

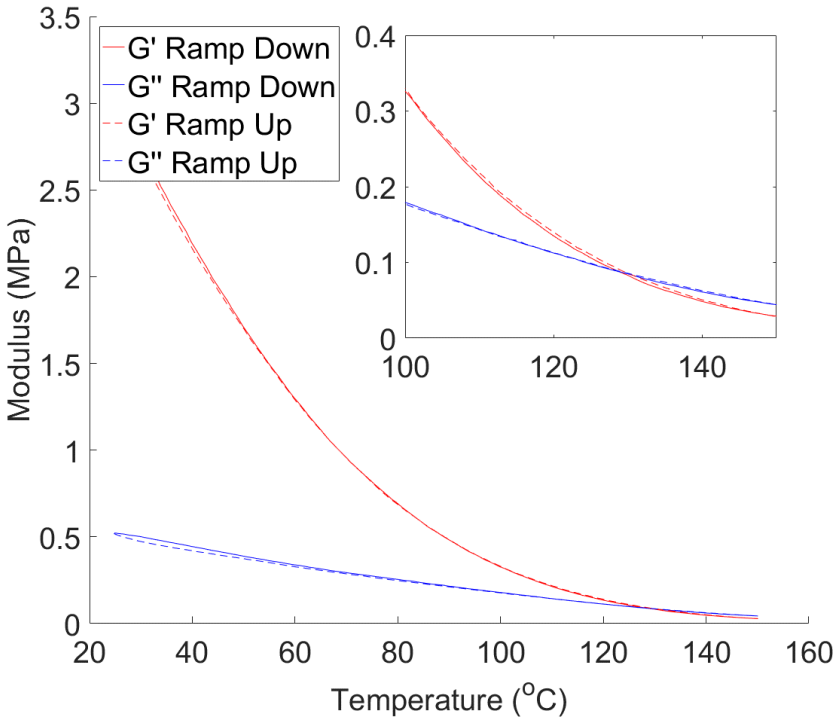

Figure 2 *The rheological data of polymer **7** from the second cool-heat cycle, with an inset showing the crossover temperature of 128 °C. See SI, S4 for other two cycles.*

Polymer degradation studies

From analysis of the fluoride initiated degradation studies conducted on a model compound (See SI, S1) the proposed scheme for degradation of polymer **7** is shown in Scheme 4, with

mechanistic break down detailed within the box. Upon addition of fluoride ions, the silyl group readily cleaves to form the *tert*-butyldimethylsilyl fluoride **8c** and a phenoxide ion. This species spontaneously degrades[44] to release carbon dioxide **8d** and the degraded polymer backbone **8a**. The quinone reacts with environmental water, resulting in the formation of cresol group **8b**.

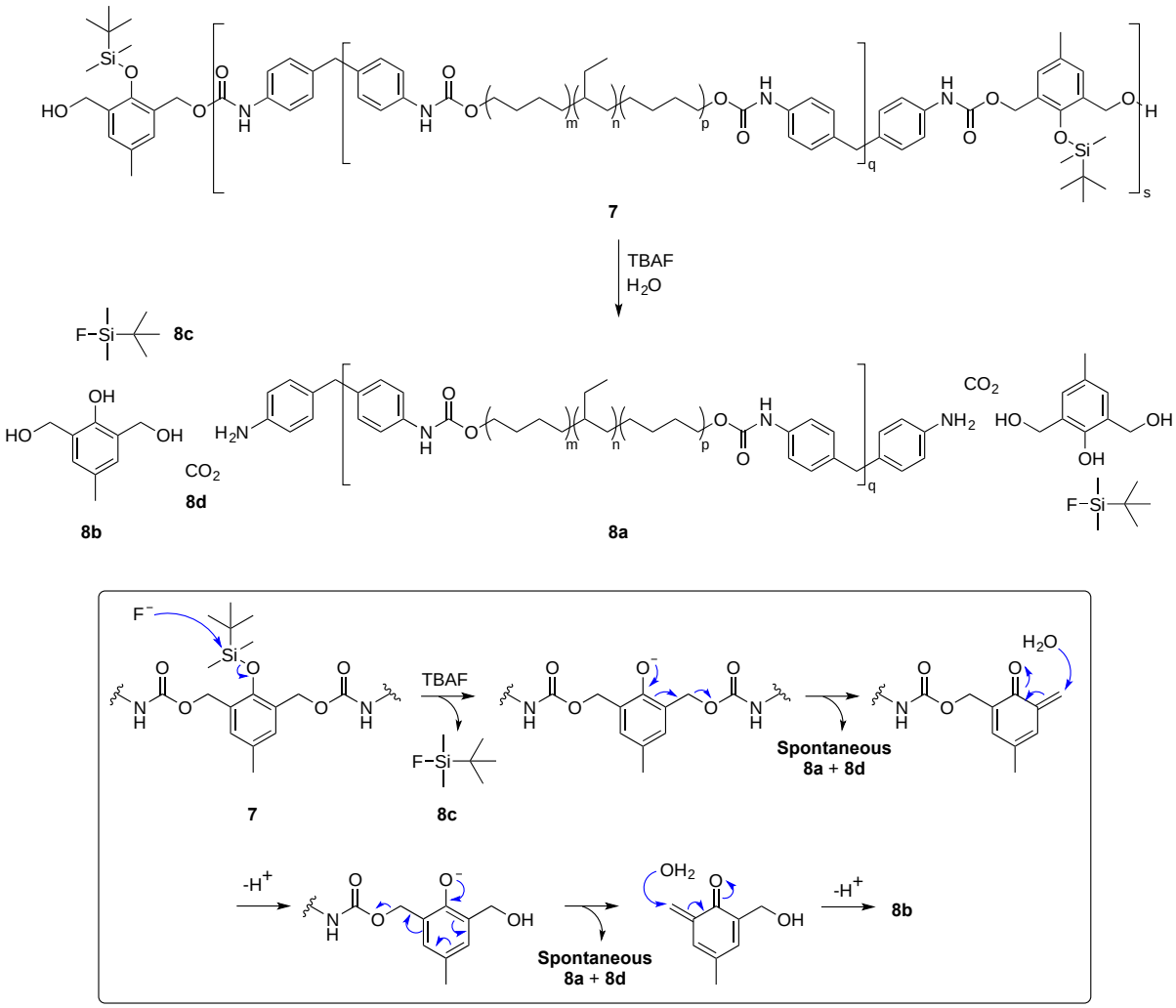

Scheme 4 *Depolymerisation of Polymer **7** after TBAF has been applied. Insert shows mechanistic break down of the degradable group within PU **7**.*

To verify fluoride initiated degradation occurred in the polymeric system, solution state studies were conducted by addition of TBAF to a sample of **7** in $CDCl_3$ (1:1 molar equivalents of TBAF to responsive unit). The degradation was monitored by ^1H NMR spectroscopy. Within 1 minute of exposure to TBAF, the methylene proton resonances at 5.18 ppm and urethane N-

H resonances at 6.60 ppm were not evident in the ^{1}H NMR spectra of the solution of polymer **7** indicating rapid and efficient degradation of the polymer (Figure 3).

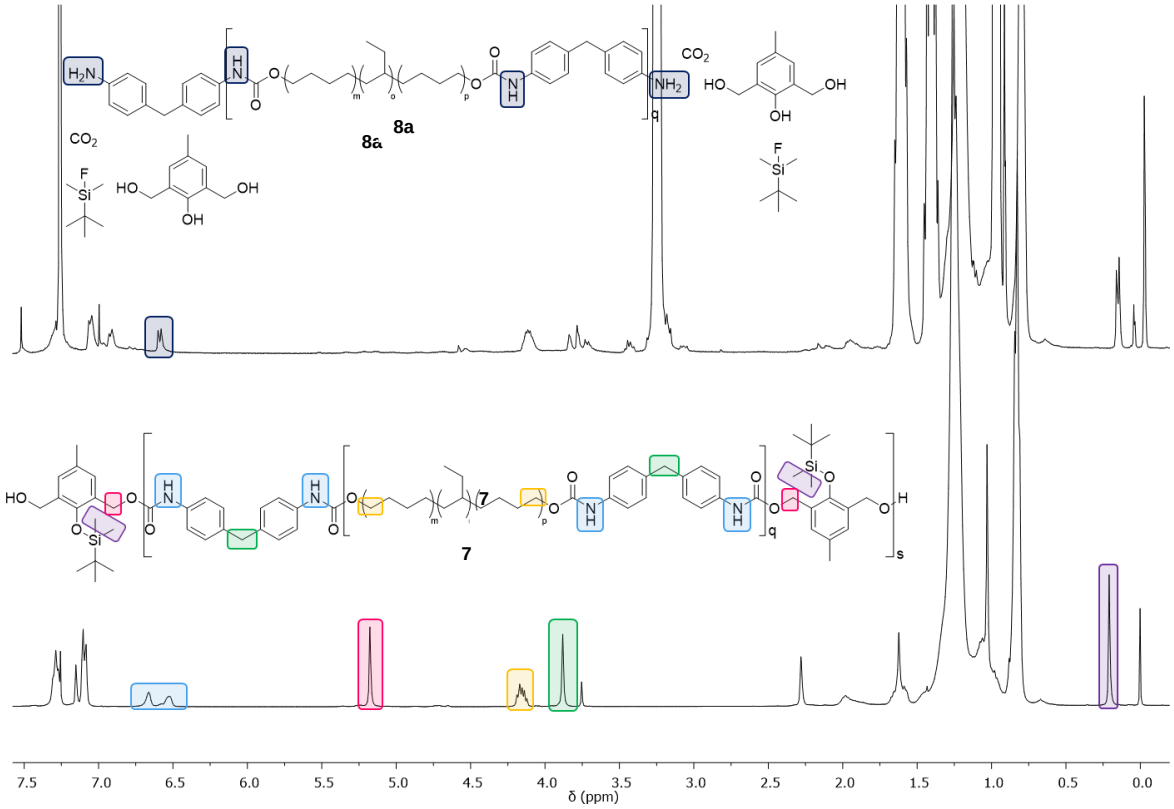

Figure 3 *^{1}H NMR spectra showing the degradation of Polymer **6** when treated with TBAF. ($CDCl_3$, 400 MHz).*

GPC eluograms of the Krasol **4**, polymer **7**, and the degraded polymer **8a** are shown in Figure 4. The eluogram for the degraded material is clearly bimodal in nature, however, the overall distribution was calculated to have M_n 6.2 kgmol^{-1} and *Đ* 1.73 (Figure 4, Table 1). This drop in molecular weight from polymer **7** (M_n = 26.1 kgmol^{-1}, *Đ* 2.73) confirms the highly efficient fluoride ion initiated degradation of the system. The bimodal appearance of the eluogram of the degraded product has signal maxima at 13 and 3.7 kgmol^{-1}. The lower M_n value may be compared to the molecular weight of the starting Krasol, (M_n = 3.3 kgmol^{-1}). The persistence of a higher molecular weight fraction in the degraded product M_n = 6.3 kgmol^{-1} can be accounted for by considering uncontrolled nature of the polymerisation (Scheme 3). This results in significant chain extension during the synthesis of prepolymer **6** (Scheme 3), where

multiple Krasol units may be connected by MDI residues which are not separated by the DU. Therefore, these Krasol-MDI-Krasol sections are not susceptible to degradation and persist in the molecular weight distribution of the degraded material. Indeed, from the GPC results, it can be estimated that the value for q in **7** (Scheme 3) and **8a** (Scheme 4) is approximately 2.

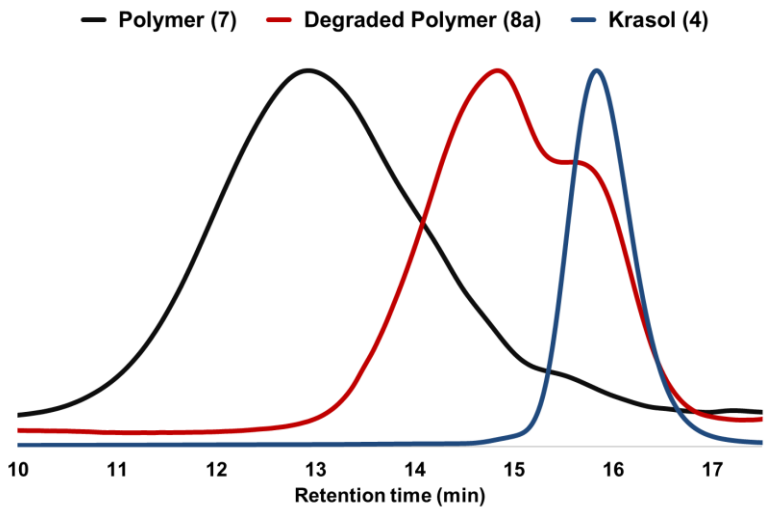

Figure 4 *GPC eluograms of polymer (**7**), degraded polymer (**8a**) and the starting Krasol (**4**); (THF, PS standards).*

Table 1 *Molecular weight estimation from the GPC chromatographs for polymer (**7**), degraded polymer (**8a**) and Krasol (**4**); (THF, PS standards).*

	M_w ($gmol^{-1}$)	M_n ($gmol^{-1}$)	*Đ*
Polymer (7)	71400	26100	2.7
Degraded Polymer (8a)	10000	6200	1.7
Krasol (4)	3700	3300	1.1

Solid state mechanical testing and degradation studies

Attention then moved on to mechanical testing of polymer **7** which could be readily cast into large (15 × 15 cm) homogeneous films. From a single casting, ten strips (4.0 × 0.5 cm) were produced of which five samples were immersed in 1M TBAF/Acetone, then dried at 40 °C for

30 minutes. The stress-strain profiles for pristine polymer **7** and the degraded polymer (**8a**) are shown in Figure 5 with numerical mechanical data summarised in Table 2.

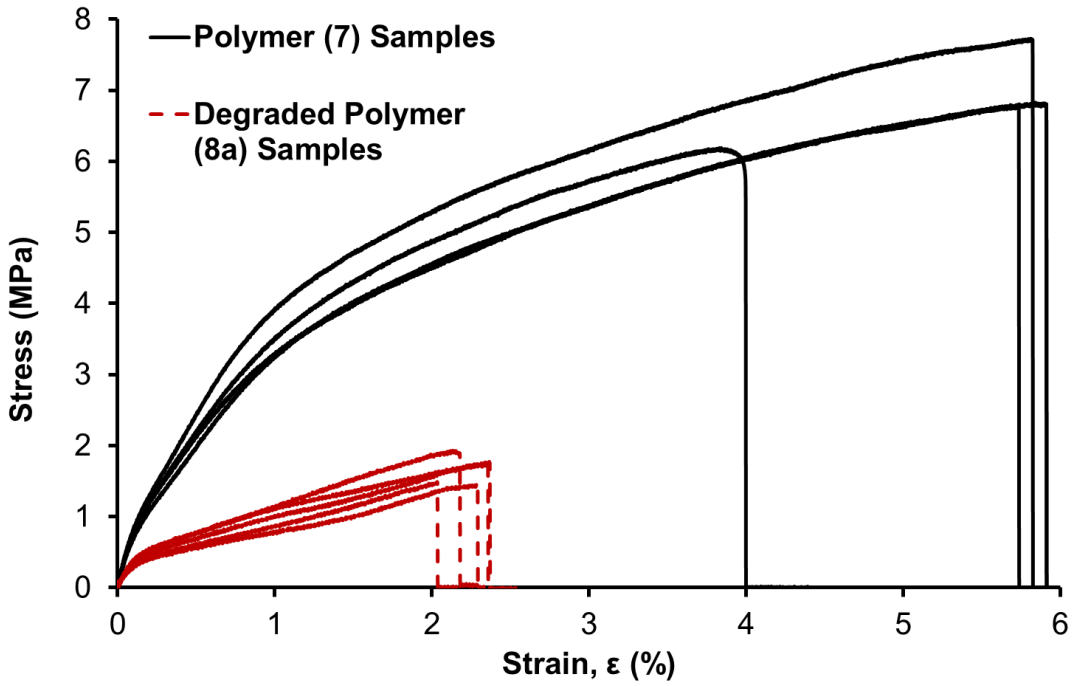

Figure 5 *Stress-strain curves for five samples of pristine polymer (**7**) and five samples of degraded polymer (**8a**). Strain (ε) has been calculated from the displacement of the sample.*

Table 2 *Mean (n = 5) mechanical properties of the pristine polymer (**7**), degraded material (**8a**). Standard deviations are shown in brakets.*

	Tensile Modulus (MPa)	**Ultimate tensile Strength (MPa)**	**Elongation at break (%)**	**Toughness (MJ m^{-3})**
Polymer (7) Samples	2.56 (0.23)	6.90 (0.55)	81 (4)	27 (5.6)
Degraded Polymer (8a) Samples	0.61 (0.14)	1.68 (0.20)	77 (2)	2 (0.4)

The testing data show that the modulus of toughness of the fluoride degraded polymer (**8a**) was just 9 % of that recorded for the pristine material **7**. The Young's modulus and ultimate tensile strength of the degraded polymer **8a** both decreased by 76 % when compared to pristine

polymer **7**. These data collectively show the dramatic effect that depolymerisation has on the physical properties of the polymer.

To assess the adhesive properties of the stimuli responsive polymer, re-bonding tests were carried out on steel nails with 3.0 mm heads that were bonded using polymer **7** for 30 minutes at 160 °C (see SI, S5).[48] Figure 6 shows the results of thermal re-adhesion experiments. In these tests, the samples were stressed to breaking point using a pull adhesion test. The separated surfaces were then placed in contact and heated again for 30 minutes at 160 °C prior to re-testing. The zero cycle result corresponds to the force required to break the pristine bond, and the subsequent cycles refer to the number of times the bond has been reformed after breaking.

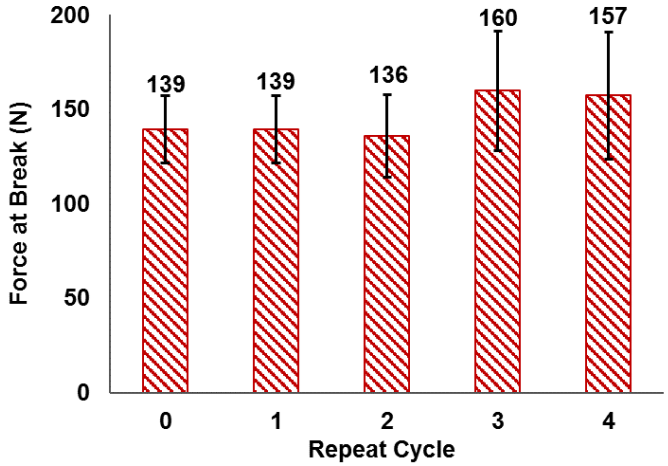

Figure 6 *Force at break after increasing bond/debond. Errors show standard deviation from the mean (n = 5).*

The consistency of the measured force at break as a function of the bond/debond cycle number confirms the reversible nature of the novel adhesive. Furthermore, the bond can be broken using heat, rather than force (see SI, video 1), and reformed again without loss in strength.

The response of the adhesive to fluoride ions was determined by placing the bonded metal surfaces in a 0.02 M TBAF/acetone solution for 3 hours and 24 hours. As evident from Figure 7, the samples that were exposed to the TBAF solution exhibited a reduction of 41% in their

force at break. After the adhesion tests, the residue of one of the TBAF degraded samples was analysed by GPC (Figure 8) which showed an average molecular weight of ~10 $kgmol^{-1}$. The slightly higher M_n value of this degraded material compared to that observed during the solution state studies (6.2 $kgmol^{-1}$, Table 1) suggests that depolymerisation is hindered in the solid state, presumable as a consequence of reduced access (low rates of diffusion) of the fluoride ions to the depolymerisation units. Minimal further change was observed in the adhesive bonds strength when in sample were allowed to degrade for more than 24 hours.

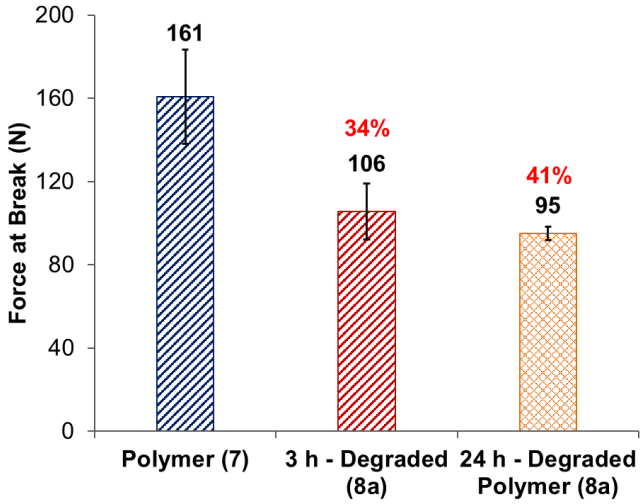

Figure 7 *The force at break of the bonded surfaces adhered with the pristine polymer and the polymer after exposure to TBAF after 3 and 24 hours. Errors show standard deviation from the mean (n = 5, 4 and 4 per experiment respectively).*

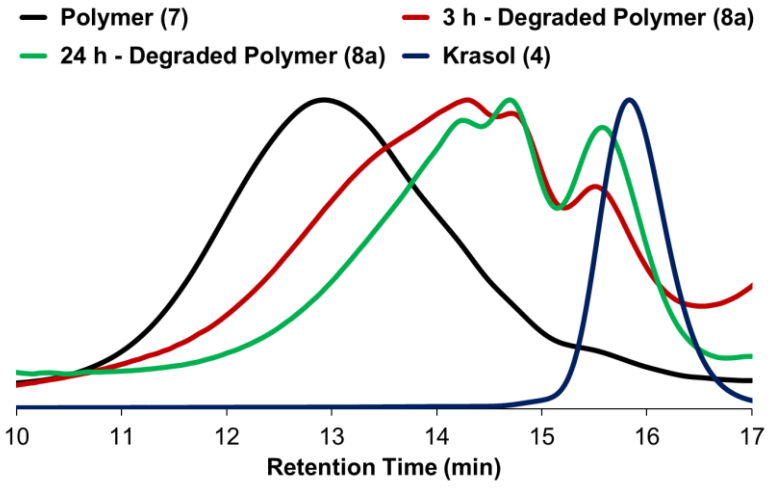

Figure 8 *GPC eluograms of the degraded polymer (**8a**) from the adhesion test compared to the pristine polymer (**7**) and Krasol (**4**).*

Table 3 *Molecular weight data from the GPC chromatographs for polymer (**7**), a sample of the degraded adhesive (**8a**) and Krasol (**4**) (THF compared to PS).*

	M_n ($gmol^{-1}$)	M_w ($gmol^{-1}$)	*Đ*
Polymer (**7**)	26100	71400	2.7
3 h – Degraded Polymer (**8a**)	10400	27300	2.6
24 h – Degraded Polymer (**8a**)	8600	19000	2.2
Krasol (**4**)	3300	3700	1.1

The irreversibility nature of the fluoride degraded adhesive was also assessed. This was investigated by thermally induced re-adhesion of the degraded polymer. Figure 9 shows the force at break measured during pull adhesion tests for metal samples re-bonded with either the pristine polymer, control samples that were exposed to acetone only, or samples that were exposed to an acetone solution of TBAF for 3 hours.

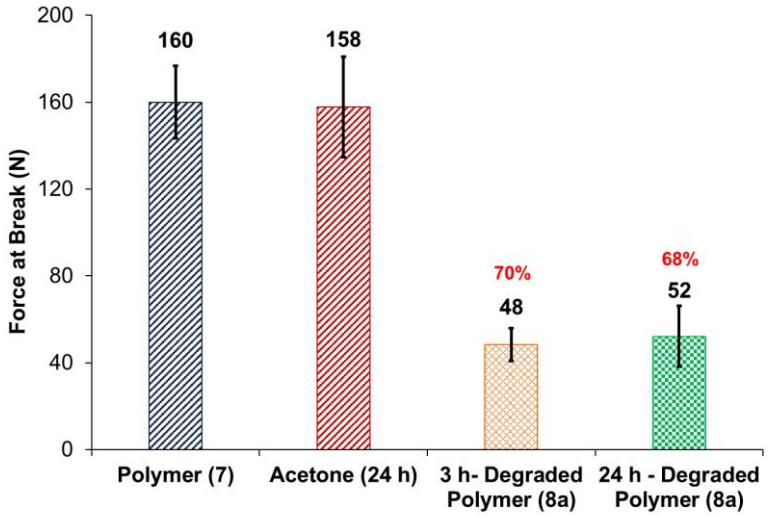

Figure 9 *Force separate the surfaces bonded with the pristine polymer (**6**), polymer **6** after exposure either acetone or a solution of TBAF in acetone. Errors show standard deviation from the mean (n = 3, 3, and 5 per experiment respectively).*

These data demonstrate that exposure to acetone has essentially no impact on the strength of the re-adhered samples. In contrast, the samples that were exposed to TBAF solution prior to being re-adhered exhibited a dramatic (70%) loss in their force at break.

Finally, to investigate the potential utility of the new adhesive with respect to bonding different substrates, lap shear tests were carried out on samples of adhered wood, glass (soda-lime) and metal (aluminium) substrates. In these tests, pristine samples were adhered with polymer **7** at 160 °C for 30 minutes prior to testing. Degradation was achieved by placing the samples in a 0.02 M TBAF acetone solution for 3 hours, prior to drying (160 °C) and testing. The maximum force before failure was recorded, and converted to lap shear stress (MPa) to account for the area of bonded polymer (Figure 10). During attempts to study the bonding strength on polyacetate (PA) substrates, the PA yielded before the adhesive failed.

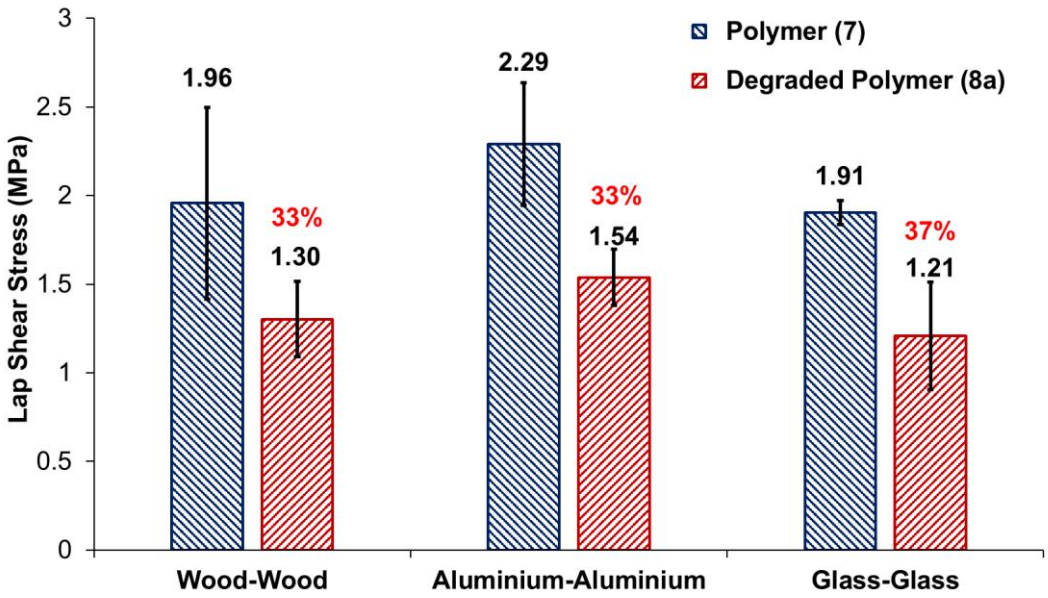

Figure 10 *Lap shear stress values of Polymer **7** between different material substrates, before and after degradation. Figures in black indicate the lap shear stress value, and red indicates the percentage of degradation in bond strength compared to the pristine material. Errors show standard deviation from the mean (n = 4 for Wood-Wood and Glass-Glass samples and n=5 for Aluminium-Aluminium samples)*

These results demonstrate that the polymer can be used to adhere several different substrate materials. Furthermore, the nature of the substrate has little effect on the loss of adhesion strength on contact with fluoride ions (*c.* 35% loss).

Conclusions

We have synthesised a novel, dicarbamate containing fluoride responsive degradable group, which can be incorporated into a linear PU using solvent free conditions. Analysis of model compound (**3**) showed that the degradable group is selectively responsive to fluoride ions (rather than other halide ions). Bond/debond tests demonstrate the linear PU behaves as a typical thermoplastic adhesive, undergoing four break/heal cycles without loss of strength. GPC and ^{1}H NMR spectroscopic studies confirm that the polymer **7** degrades in the both the solvent and solid state on the addition of fluoride ions. Pull tensile adhesion studies also showed bonded surfaces exhibit 40% loss of adhesion strength after the system is exposed to a fluoride source. The adhesive can be used to bond multiple different surfaces including wood, acetate and aluminium.

Experimental Section

Materials. Krasol HLBH-P2000 was kindly supplied by Cray Valley. 2,6-Bis(hydroxymethyl)-*p*-cresol, *tert*-butyldimethylsilyl chloride and imidazole were purchased from Alfa Aesar and used as received. All other chemicals were purchased from Sigma-Aldrich and used as received.

Characterisation. ^{1}H NMR and ^{13}C NMR spectra were recorded on either a Bruker Nanobay 400 or a Bruker DPX 400 spectrometer operating at 400 MHz for ^{1}H NMR or 100 MHz for ^{13}C NMR, respectively. The samples for NMR spectroscopic analysis were prepared in $CDCl_3$ or DMSO, and dissolution was aided with slight heating. The data was processed using MestReNova Version 6.0.2-5475. Chemical shifts (δ) are reported in ppm relative to tetramethylsilane (δ 0.00 ppm) for $CDCl_3$ and the residual solvent peak (δ 2.50 ppm) for d_6-DMSO in ^{1}H NMR spectra. ^{13}C NMR spectroscopy was carried out using $CDCl_3$ and reported relative to chloroform (δ 77.0 ppm). ^{1}H NMR coupling constants (J) are expressed in hertz

(Hz). Infrared spectroscopic analysis was carried out on a PerkinElmer 100 FT-IR spectrometer equipped with a diamond ATR sampling attachment, and samples were analysed in neat form. The infrared spectroscopic data were processed using Microsoft Excel 2016. Ultraviolet-visible spectroscopy was conducted using a Varian Cary 300 spectrophotometer with heating attachment, using a 1 cm^3 quartz cuvette, in the wavelength range 200 – 800 nm. The UV-visible spectroscopic data were processed using Microsoft Excel 2016 Gel permeation chromatography (GPC) was conducted using an Agilent Technologies 1260 Infinity systems and the data were processed using Agilent GPC/SEC software; polystyrene was used as the calibrant. Samples for GPC analysis were dissolved in analytical grade THF (2 mg/mL) with butylated hydroxytoluene (BHT) stabiliser, and run using the same solvent as the mobile phase; eluting through two Agilent PLgel 5µm MIXED-D 300 × 7.5 mm columns in series. Differential scanning calorimetric analysis used a TA Instruments DSC 2920, and a seven cycle process was carried out on the solid sample: heating from ambient to +100 °C at a ramp rate of 10 °C min^{-1}, followed by cooling from +100 °C to −70 °C at a ramp rate of −5 °C min^{-1} and then finally by heating from −70 °C to +200 °C at a ramp rate of +5 °C min^{-1}, with the previous two cycles repeated twice. The sample size used was 5-6 mg, and the data was processed using TA Universal Analysis Version 4.7A and Microsoft Excel 365 . Thermogravimetric analysis employed a TGA Q50 instrument by heating the solid samples (sample size *ca*. 20 mg) from ambient temperature to +300 °C at a ramp rate of +10 °C min^{-1}. The data was processed using TA Universal Analysis Version 4.7A. Tensile and Adhesion tests were carried out using an AML X5-500 single column universal tester, attached with a 5 kN load cell and wedge grips. Samples were analysed at a strain rate of 100mm/min (0.0656 s^{-1}).

Rheological assessment was conducted using an Anton Paar Physica MCR 301 rheometer with a parallel plate oscillatory shear set-up. Circular samples of 25 mm diameter (0.35 mm average thickness) were cut from the polymer film using a steel punch cutter. For the single frequency temperature sweep, samples were placed into the rheometer and initialised at 150 °C and then subjected to temperature ramp cycle at a rate of 2 °C/min down to 25 °C and back up at the same rate to 150 °C. This cycle was repeated two more times to assess repeatability and any changes in properties. The frequency of oscillation was set to 5 Hz, and the shear strain amplitude to 0.1%. Dynamic shear moduli (G', G'', tan δ) were recorded to characterise the material.

The DMA employed a TA instruments Q800 DMA using a tension (film/fibre) clamp. Full calibration was performed for the clamp prior to testing according to the protocol defined by

TA. The polymer sample dimensions were gauge length (defined by the clamp spacing) = 12.8 mm, width = 5.5 mm, thickness = 0.33 mm. A frequency sweep (0.5, 2, 5, 10 Hz) was performed at 2 °C temperature steps from -75 °C to 130 °C, equilibrating for 3 min at each temperature step before the storage and loss moduli data (E' and E'') were recorded.

The data for both analyses were processed first using TA Universal Analysis Version 4.5A, followed by Matlab version R2016a.

Lap shear tests: The wood and metal coupons were 7 × 30 mm, with an overlap of 7 mm; and the glass coupons were 25 × 70 mm, with an overlap of 10 mm. The coupons were washed with methanol prior to use to remove any contaminants.

Synthesis of DU 2

To a solution of 2,6-bis(hydroxymethyl)-*p*-cresol (27.50 g, 0.163 mmol) in anhydrous *N*,*N*'-dimethylformamide (500 mL), imidazole (44.52 g, 0.654 mmol) and *tert*-butyldimethylsilyl chloride (98.57 g, 0.654 mmol) was added and stirred at 35 °C for 18 hours. The mixture was diluted with ethyl acetate (500 mL) and washed with deionised water (2 x 500 mL).The organic solution was dried over $MgSO_4$, filtered and concentrated to afford an orange/brown oil; which was dissolved in 50:50 methanol : diethyl ether mixture (400 mL) and *p*-toluenesulfonic acid (4.00 g, 2.32 mmol) was added and stirred at ambient temperature for 1 hour. The mixture was diluted in ethyl acetate (300 mL) and washed with saturated Na_2CO_3 solution (300 mL) followed by brine solution (300 mL), dried over $MgSO_4$ and concentrated to afford a pale yellow/orange oil; which was dissolved in chloroform (100 mL) and precipitated slowly into cooled hexane (900 mL). The precipitate was filtered and allowed to dry under vacuum to afford a white powder (20.10 g, 48 %). ν_{max} (solid, cm^{-1}) 3220, 2961, 2926, 2881, 2857, 1453, 1221, 905, 776. δ_H (400 MHz, $CDCl_3$, ppm) 7.14 (2H, Ar-H), 4.65-4.64 (4H, d, *J* = 5.5 Hz, Ar-C$\underline{H}_2$OH), 2.30 (3H, Ar-CH_3), 1.57 (2H, Ar-$CH_2O\underline{H}$), 1.03 (9H, $C(CH_3)_3$), 0.19 (6H, $Si(CH_3)_2$). δ_C (100 MHz, $CDCl_3$, ppm) 147.9, 131.8, 131.7, 129.1, 61.2, 26.0, 20.6, 18.7, 0.0, -3.7. (m/z) 305.15 Da ($C_{15}H_{26}O_3NaSi$), calculated 305.15 Da ($C_{15}H_{26}O_3NaSi$)

Synthesis of Polymer 7

Krasol HLBH-P 2000 was dried in a vacuum oven at 100 °C and 100 mbar. 4,4'-Methylene diphenyl isocyanate (5.00 g, 20.0 mmol) was added to Krasol HLBH-P2000 (21.00 g, 10.0 mmol) and stirred at 60 rpm, 80 °C for 3 hours. The reaction temperature was raised to 100 °C and DU **2** (2.82 g, 10.0 mmol) was added and stirred for 1 hour. The crude polymer was

dissolved in chloroform (100 mL) and precipitated slowly into methanol (900 mL). The precipitate was filtered and washed with methanol (2 × 100 mL) to remove excess impurities. The precipitate was dissolved in tetrahydrofuran (100 mL) and concentrated to afford a clear white/yellow polymer (27.6 g, 96 %). δ_H (400 MHz, $CDCl_3$, ppm) (n = number of chain extension) 7.38 – 7.20 (m, $8H_n$), 7.21 – 7.02 (m, $8H_n + 2H_n$), 6.55 (m, $4H_n$), 5.17 (s, $4H_n$), 4.82 – 4.59 (m, $0.3H_n$), 4.23 – 4.07 (m, $4H_n$), 3.88 (s, $4H_n$), 2.30 (m, $3H_n$), 1.93 – 0.71 (m, $350H_n$), 0.21 (s, $6H_n$). δ_C (100 MHz, $CDCl_3$, ppm) 153.7, 153.5, 149.16, 136.3, 136.2, 136.1, 135.9, 131.4, 130.8, 129.4, 126.9, 118.9, 62.5, 40.6, 38., 38.7, 38.4, 38.1, 37.9, 37.3, 36.1, 34.9, 33.5, 33.3, 30.7, 30.5, 30.2, 29.9, 29.8, 29.3, 26.8, 26.6, 26.5, 26.1, 25.9, 25.9, 20.6, 19.5, 18.7, 11.4, 10.9, 10.7, 10.66, 10.6, 9.4, 0.0, -0.9, -3.7. GPC (THF/BHT 250 ppm) M_w 71400, M_n 26100, *Đ* 2.73.

Sample Preparation Mechanical Assessment. A thin film of the polyurethane was produced for mechanical testing via a solution casting procedure. The polyurethane was dissolved in THF, and the solution was poured into a flat PTFE mold. The solvent was allowed to evaporate slowly at room temperature and pressure overnight, then at 50 °C with a pressure of approximately 800 mbar for a duration of 24 hours. Polyurethane film of uniform thickness between 200 and 500 μm was obtained at the end of this procedure without residual solvent. For tensile testing, rectangular samples of approximately 4.0 cm × 0.5 cm were cut with a blade, and paper end-tabs were used between the grips and the polymer sample. This sample assembly was found to reduce slippage and/or tearing inside the tensile grips of the tensiometer.

Acknowledgements
The authors would like to thank AWE Plc and the ESPRC for co-funding a studentship for TSB. We are grateful to the University of Reading for access to instrumentation in the Chemical Analysis Facility, and the Department of Engineering Science at the University of Oxford for use of their Rheometer and Dynamic Mechanical Analyser, and Cray Valley for the supply of Krasol HLBH-P2000. AT's research is supported by the Air Force Office of Scientific Research, Air Force Material Command, USAF under Award No. FA9550-15-1-0448

Associated Content
The Supporting Information is available free of charge on the "website" at DOI "####".
Experimental details for synthesis of the model bisurethane compound; selectivity of the silyl model compound to fluoride ions, compared to other halide ions followed by ^{1}H NMR spectroscopy; experimental details of the synthesis of methoxy analogue and its corresponding model compound, followed by degradation studies followed by ^{1}H NMR spectroscopy; UV-visible spectroscopic studies of the model compound before and after degradation; Differential Scanning Calorimetry; Rheometric Analysis and Dynamic Mechanical Analysis; Temperature

dependant adhesive bond strengths; ^{1}H and ^{13}C NMR spectroscopic characterisation of the DU, model bisurethane compound and polymer. Video of the thermal debonding of the adhesive.

Author Information

Corresponding Author:
B. W. Greenland: Email: b.w.greenland@sussex.ac.uk

Notes:
The authors declare no competing financial interest.

References

1. F. Awaja, M. Gilbert, G. Kelly, B. Fox and P. J. Pigram, *Prog. Polym. Sci.*, 2009, **34**, 948–968.
2. F. Chabert, F. Tournilhac, N. Sajot, S. Tenc-Girault and L. Leibler, *Int. J. Adhes. Adhes.*, 2010, **30**, 696–705.
3. J. A. Pomposo, J. Rodrıguez and H. Grande, *Synth. Met.*, 1999, **104**, 107–111.
4. C. Galan, C. A. Sierra, J. M. Gomez Fatou and J. A. Delgado, *J. Appl. Polym. Sci.*, 1996, **62**, 1263–1275.
5. M. Fernandez, M. Landa, M. E. Munoz and A. Santamaria, *Macromol. Mater. Eng.*, 2010, **295**, 1031–1041.
6. X. Luo, K. E. Lauber and P. T. Mather, *Polymer*, 2010, **51**, 1169–1175.
7. A. Bakken, N. Boyle, B. Archambault, A. Hagen, N. Kostry, K. Fischer and R. Taleyarkhan, *Int. J. Adhes. Adhes.*, 2016, **71**, 66–73.
8. J. Canales, M. E. Muñoz, M. Fernández and A. Santamaría, *Compos. PART A*, 2016, **84**, 9–16.
9. C. W. Peak, J. J. Wilker and G. Schmidt, *Colloid Polym. Sci*., 2013, **291**, 2031–2047.
10. G. Sudre, L. Olanier, Y. Tran, D. Hourdet and C. Creton, *Soft Matter*, 2012, **8**, 8184–8193.
11. C. Ghobril and M. W. Grinstaff, *Chem. Soc. Rev.*, 2015, **44**, 1820–1835.
12. B. M. Shin, J. Kim and D. J. Chung, *Macromol. Res.*, 2013, **21**, 582–587.
13. E. M. White, J. E. Seppala, P. M. Rushworth, B. W. Ritchie, S. Sharma and J. Locklin, *Macromolecules*, 2013, **46**, 8882−8887.
14. J. H. Aubert, *J. Adhes*., 2003, **79**, 609–616.
15. S. N. Ghosh and S. Maiti, *J. Appl. Polym. Sci.*, 1997, **63**, 683–691.
16. K. Luo, T. Xie and J. Rzayev, *J. Polym. Sci. Part A Polym. Chem.*, 2013, **51**, 4992–4997.
17. Q. Zhang, M. Molenda and T. M. Reineke, *Macromolecules*, 2016, **49**, 8397–8406.

18. U. Lafont, H. Van Zeijl and S. Van Der Zwaag, *ACS Appl. Mater. Interfaces*, 2012, **4**, 6280–6288.

19. Z. Czech, *J. Adhes. Sci. Technol.*, 2007, **21**, 625–635.

20. H. Chung and R. H. Grubbs, *Macromolecules*, 2012, **45**, 9666–9673.

21. R. J. Wojtecki, M. a Meador and S. J. Rowan, *Nat. Mater.*, 2011, **10**, 14–27.

22. C. Heinzmann, S. Coulibaly, A. Roulin, G. L. Fiore and C. Weder, *ACS Appl. Mater. Interfaces*, 2014, **6**, 4713–9.

23. S. T. Phillips, W. Seo, J. S. Robbins, M. Olah, K. Schmid, A. M. DiLauro, WO2012005806 A2, 2012.

24. P. J. M. Bouten, M. Zonjee, J. Bender, S. T. K. Yauw, H. Van Goor, J. C. M. Van Hest and R. Hoogenboom, *Prog. Polym. Sci.*, 2014, **39**, 1375–1405.

25. V. Delplace and J. Nicolas, *Nat. Chem.*, 2015, **7**, 771–784.

26. Y. Shi, P. Zhou, R. Freitag and S. Agarwal, *ACS Biomater. Sci. Eng.*, 2015, **1**, 971–977.

27. S. Ho and A. M. Young, *Eur. Polym. J.*, 2006, **42**, 1775–1785.

28. H. Mohapatra, H. Kim and S. T. Phillips, *J. Am. Chem. Soc.*, 2015, **137**, 12498–12501.

29. B. T. Michal, E. J. Spencer and S. J. Rowan, *ACS Appl. Mater. Interfaces*, 2016, **8**, 11041–11049.

30. P. Pissis, G. Georgousis, C. Pandis, P. Georgiopoulos, A. Kyritsis, E. Kontou, M. Micusik, K. Czanikova and M. Omastova, *Procedia Engineering*, 2015, **114**, 590–597.

31. Z. Guo, Y. Zuo and S. Feng, *RSC Adv.*, **6**, 73140–73147.

32. E. Chaberta, J. Vialb, J.-P. Cauchoisc, M. Mihaluta and F. Tournilhaca, *Soft Matter*, 2016, **12**, 4838–4845.

33. M. A. Ayer, Y. C. Simon and C. Weder, *Macromolecules*, 2016, **49**, 2917–2927.

34. J. Lai, J. Mei, X. Jia, C. Li and X. You, *Adv. Mater.*, 2016, **28**, 8277–8282.

35. C. Heinzmann, C. Weder and L. M. de Espinosa, *Chem. Soc. Rev.*, 2015, **342**, 342–358.

36. A. Faghihnejad, K. E. Feldman, J. Yu, M. V. Tirrell, J. N. Israelachvili, C. J. Hawker, E. J. Kramer and H. Zeng, *Adv. Funct. Mater.*, 2014, **24**, 2322–2333.

37. K. A. Houton, G. M. Burslem and A. J. Wilson, *Chem. Sci.*, 2015, **6**, 2382–2388.

38. C. Heinzmann, U. Salz, N. Moszner, G. L. Fiore and C. Weder, *ACS Appl. Mater. Interfaces*, 2015, **7**, 13395–13404.

39. K. Yamauchi, J. R. Lizotte and T. E. Long, *Macromolecules*, 2003, **36**, 1083–1088.

40. S. Cheng, M. Zhang, N. Dixit, R. B. Moore and T. E. Long, *Macromolecules*, 2012, **45**, 805–812.

41. K. Yamauchi and A. Kanomata, *Macromolecules*, 2004, **37**, 3519–3522.

42. H. Kim, H. Mohapatra and S. T. Phillips, *Angew.Chem. Int.Ed*., 2015, **54**, 13063–13067.

43. I. S. Turan and E. U. Akkaya, *Org. Lett.*, 2014, **16**, 1680–1683.

44. M. Shamis, H. N. Lode, and D. Shabat, *J. Am. Chem. Soc.*, 2004, **126**, 1726-1731.

45. P. J. Woodward, D. Hermida Merino, B. W. Greenland, I. W. Hamley, Z. Light, A. T. Slark and W. Hayes, *Macromolecules*, 2010, **43**, 2512–2517.

46. A. Feula, X. Tang, I. Giannakopoulos, A. M. Chippindale, I. Hamley, F. Greco, C. P. Buckley, C. R. Siviour and W. Hayes, *Chem. Sci*., 2016, **7**, 4291–4300.

47. A. Feula, A. Pethybridge, I. Giannakopoulos, X. Tang, A. Chippindale, C. R. Siviour, C. P. Buckley, I. W. Hamley and W. Hayes, *Macromolecules*, 2015, **48**, 6132–6141.

48. Samples Did Not Adhere at 80 °C, and Weakly Adhered at 120 °C. See SI, S5.

Table of Contents Graphic